

# Seafloor hydrothermal systems

M.Geo.239

29 Jan 2020

Elco Luijendijk,

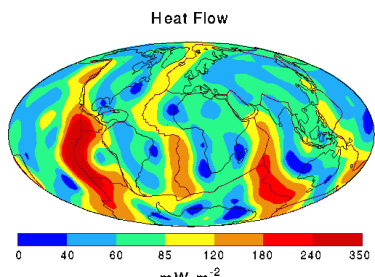
with help from Carol Stein

[eluijen@gwdg.de](mailto:eluijen@gwdg.de)

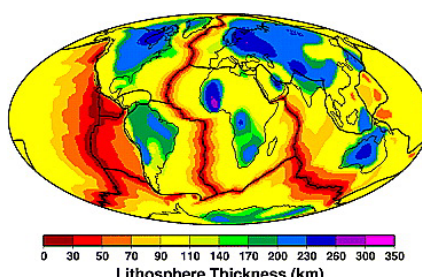


## Global heat flow and lithosphere thickness

- High heat flow due to thin crust and lithosphere near spreading ridges
- Lithosphere-asthenosphere boundary  $\sim 1300$  °C isotherm



Global heat flow, Pollack ea.  
(1993) Rev. Geophys.

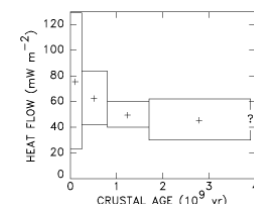
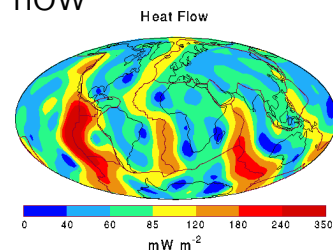


Lithosphere thickness, Conrad &  
Lithgow-Bertelloni (2006) GRL

3

## Global heat flow

- Median heat flow continental crust =  $65 \text{ mW m}^{-2}$
- Median heat flow oceanic crust =  $101 \text{ mW m}^{-2}$
- Global heat loss =  $44 \text{ TW}$
- Heat loss: 70 % at oceans, 30 % at continents
- Question: Why is oceanic heat flow higher?

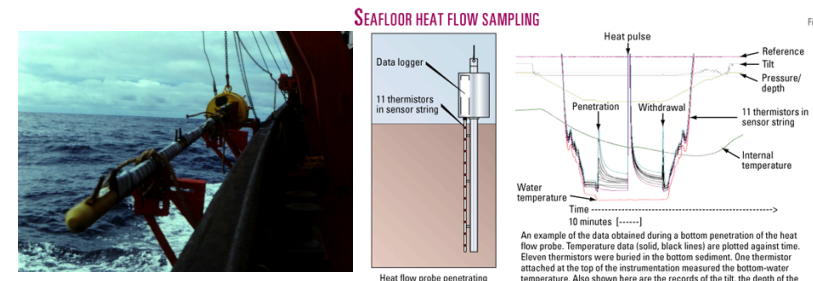


Global heat flow (top, Pollack ea (1994)) and heat flow vs age of the crust (bottom, Sclater ea (1980))

2

## Measuring oceanic heat flow

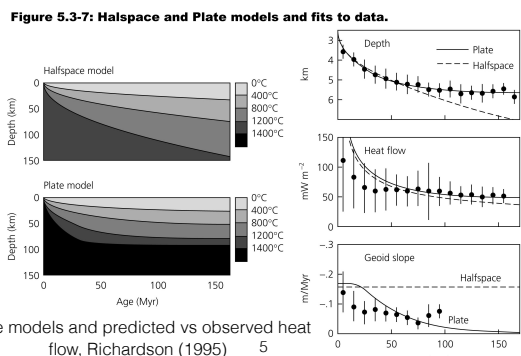
- Measuring heat flow (temperature gradient + thermal conductivity) in seafloor sediments



4

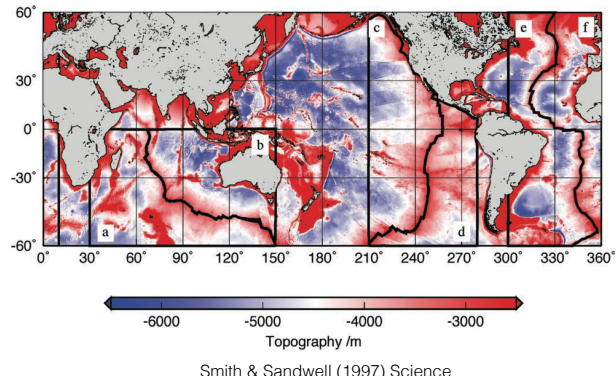
## Heat flow oceanic crust

- First order oceanic heat flow, plate thickness and depth are well predicted by models of a cooling oceanic plate
- Plate cools as it moves away from mid-oceanic ridge. cooling= increasing density = increasing depth due to isostasy
- Two competing models. The plate model by Stein and Stein (1992) does the best job of predicting depth of oceanic crust and heat flow using a purely conductive heat flow model, with an empirically fitted maximum depth of the lithosphere



## Topography oceanic crust

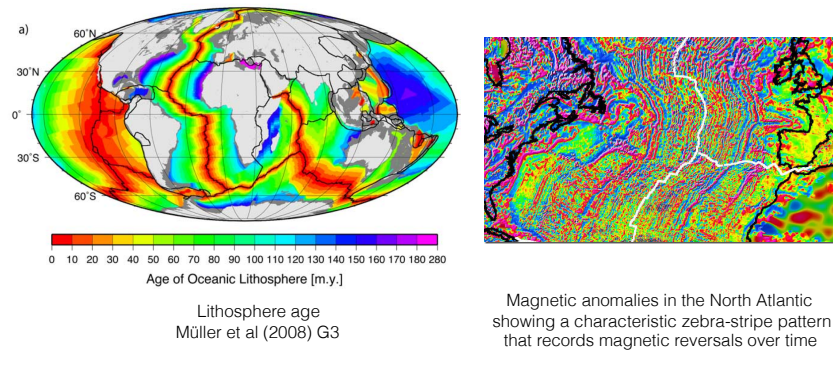
- Topography oceanic crust: function of distance to mid-oceanic ridge & age



7

## Topography oceanic crust

- Age of oceanic lithosphere, known from paleo-magnetic data



Magnetic anomalies in the North Atlantic showing a characteristic zebra-stripe pattern that records magnetic reversals over time

6

## Seafloor spreading and plate tectonics

- Observations of seafloor topography and magnetic reversals led to the theory of seafloor spreading in the 1950s
- Combination with data on subduction zones and plate motion led to the birth of the theory of plate tectonics in 1968 in a publication by Jason Morgan
- You can find the paper here: <http://onlinelibrary.wiley.com/doi/10.1029/JB073i006p01959/full>

JOURNAL OF GEOPHYSICAL RESEARCH Vol. 73, No. 6, MARCH 15, 1968

### Rises, Trenches, Great Faults, and Crustal Blocks<sup>1</sup>

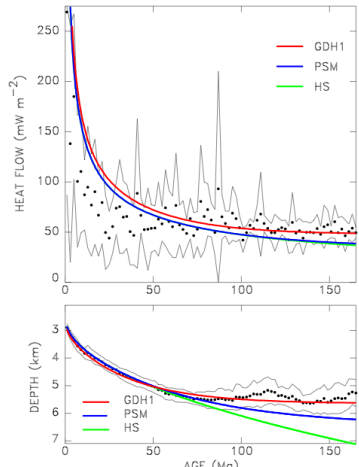
W. JASON MORGAN

Department of Geology, Princeton University, Princeton, New Jersey 08540  
and Department of Geology and Geophysics, Woods Hole Oceanographic Institution  
Woods Hole, Massachusetts 02543



## Heat flow oceanic crust

- Oceanic plate cools and depth increases as plate moves away from spreading ridge
- First order heat flow trend well matched by plate model (GDH1)
- Large scatter in observed heat flow data: spatial variability, probably a result of secondary processes

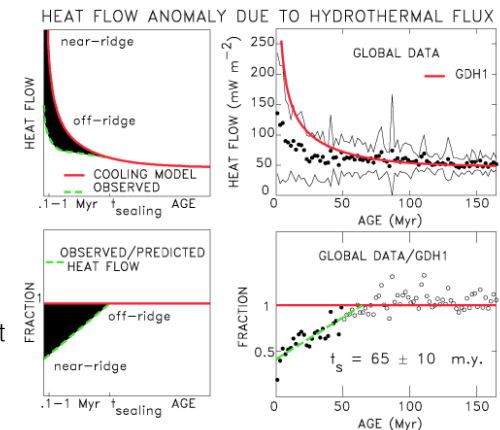


Modelled vs observed heat flow in the oceanic crust.  
9

Stein & Stein (1992) JGR

## Heat flow anomalies in oceanic crust

- However, observed heat flow much lower than predicted conductive heat flow for young ( $\sim < 65 \text{ Ma}$ ) oceanic crust
- 30% of total heat loss unexplained by any models of oceanic heat flow



Heat flow anomalies in oceanic crust. Stein & Stein, 1994, JGR  
10

## Seafloor hydrothermal vents

- Additional heat transport process in oceanic crust speculated since the 1960s
- Additional clues: occurrence of metal-rich sediments in the Red Sea rift and around mid ocean ridges, and wide zones of excess (mantle)  $^3\text{He}$
- Solved with the discovery of first high temperature seafloor hydrothermal vent in 1979 on the east-Pacific rise



Alvin: the submarine used to discover the first black smoker in 1979



The first black-smoker chimney ever seen by humans—photographed at 21°N in 1979.

11

## Seafloor hydrothermal vents

- Black smokers. High temperature ( $>350^\circ\text{C}$ ) focussed fluid discharge. Black plume is caused by metal sulphide and oxide
- Located on oceanic ridges, back arcs
- Builds up chimneys consisting of hydrothermal mineral deposits

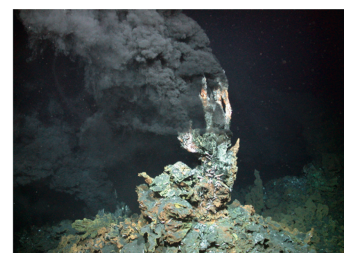
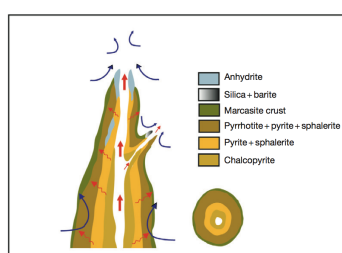


Figure 4 Photograph of a 'black smoker' hydrothermal vent emitting hot ( $>350^\circ\text{C}$ ) fluid at a depth of  $\sim 3000 \text{ m}$  into the base of the oceanic water column at the Logatchev hydrothermal field, northern Mid-Atlantic Ridge. Photograph courtesy of MARUM, Bremen, DE.

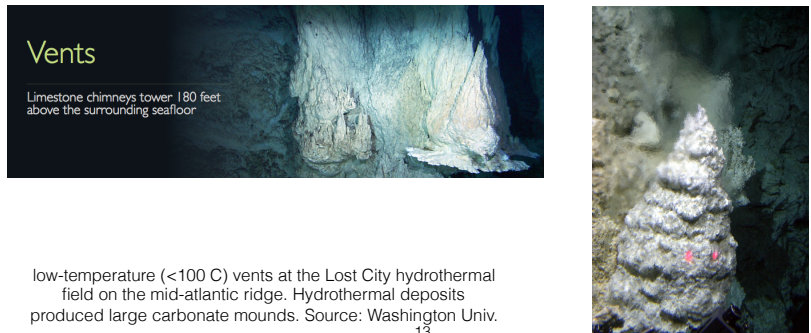


agram showing mineral zonation in cross section and in plan view for a typical black-smoker chimney (after Haymon, 1 of inferred fluid flow.

12

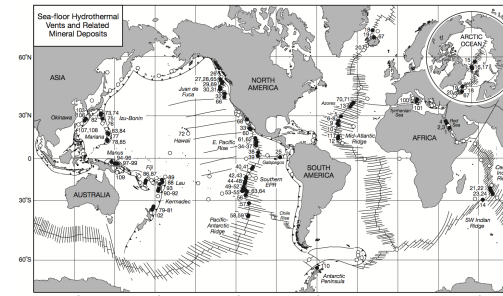
## Seafloor hydrothermal vents

- Off-axis systems in older oceanic crust:
- White smokers: moderate temperature systems (100-300 °C)
- Diffuse low-temperature (100°C) discharge -> dominant in older oceanic crust, accounts for large fluid and heat fluxes overall, but poorly known



## Seafloor hydrothermal systems

- Hydrothermal vents & associated mineral deposits are widespread, new sites discovered regularly

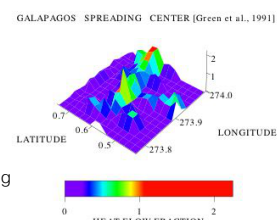
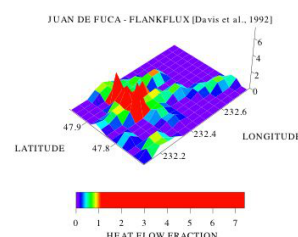


Overview of seafloor hydrothermal vents and mineral deposits. closed circles: high T systems, open circles: low T systems. Source: Hannington et al. (2005) Econ. Geology

14

## Heat flux at spreading ridges

- Result of focused hydrothermal systems: highly heterogeneous and focused heat flux
- Heat flow highs were missed previously, but calculations show that they can balance the discrepancy between observed and predicted heat flow in oceanic crust
- Extremely high heat flow at vents and high distance between vents suggest that they 'harvest' the background heat flow from large areas (10s of km<sup>2</sup>)

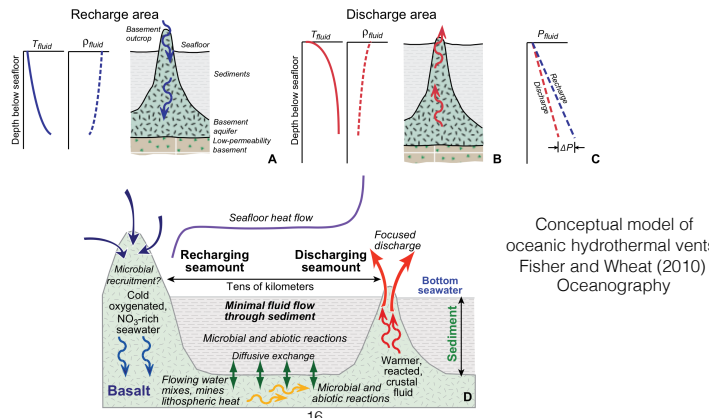


Spatial distribution of heat flux at spreading ridges (Stein & Stein, 1997)

15

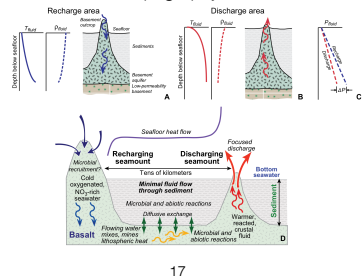
## Seafloor hydrothermal systems

- How do seafloor hydrothermal systems work?
- Off-axis hydrothermal systems in (somewhat) older oceanic crust:



## Seafloor hydrothermal systems

- Question: Can seafloor topography be a driving force for fluid flow?
  - fluid potential =  $P + \rho g z$
  - high seamount: low pressure, thinner water column (P), high elevation/gravitational potential ( $\rho g z$ )
  - low seamount: high pressure (P) but lower elevation ( $\rho g z$ )
  - > these effects cancel out, so no topography-driven flow as on land

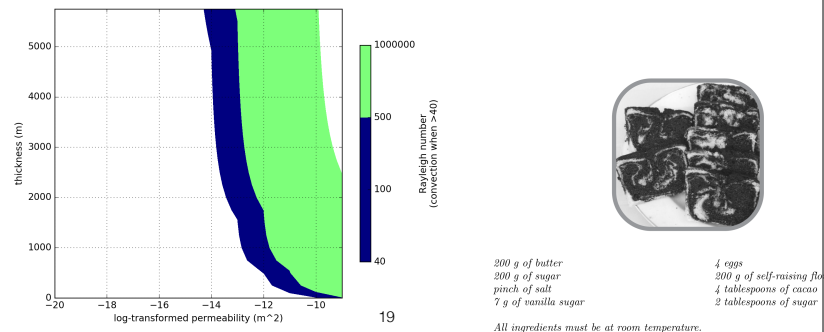


17

Conceptual model of oceanic hydrothermal vents, Fisher and Wheat (2010) Oceanography

## Seafloor hydrothermal systems

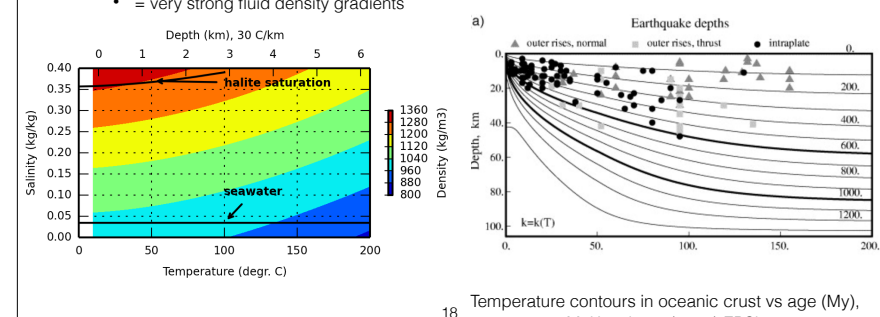
- Question: can we calculate the potential for convection?
- Rayleigh convection number:  $Ra = \frac{\alpha \rho_f^2 c_f g k L \Delta T}{\mu \kappa}$
- $\alpha$  = thermal expansion coefficient,  $\rho$ =density,  $c$ =heat capacity,  $k$ =permeability,  $L$ =length of the system,  $\Delta T$ =temperature difference,  $\mu$ =dynamic viscosity,  $K$ =thermal conductivity
- Rayleigh number for newly formed oceanic crust:  $\Delta T = 1200^\circ\text{C}$ , thickness  $L=6000\text{ m}$
- Convection at  $Ra > 40$ ,  $\log k > -14$



19

## Seafloor hydrothermal systems

- Question: What other driving forces of fluid flow could explain flow in young oceanic crust?
  - Density-driven flow?
  - fluid potential =  $P + \rho g z$
  - geothermal gradients in young oceanic crust up to  $200^\circ\text{C}/\text{km}$
  - = very strong fluid density gradients



18 Temperature contours in oceanic crust vs age (My), McKenzie ea (2005) EPSL

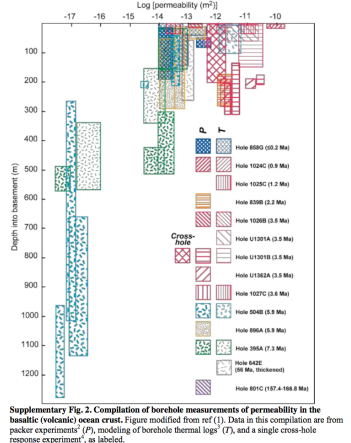
## Permeability of seafloor hydrothermal systems

- Permeability of seafloor hydrothermal systems
  - Question: Which lithology would have the highest permeability: the basement or the overlying sediments?
  - basement: basalts -> fractured because of volume changes during cooling. Permeability largely unknown, estimated from hydrothermal model studies and some in-situ tests. Upper layer of extrusive basalts is thought to be the most permeable
  - sediments: low-energy depositional environment -> fine grained pelagic carbonates and clays -> low permeability. Absent on spreading ridges, increasing coverage at older oceanic crust

20

## Permeability of seafloor hydrothermal systems

- Permeability of the oceanic basement: relatively high values in the upper ~300 m



21

Winslow et al. (2015) Nature Comm.

## Permeability of seafloor hydrothermal systems

- Global distribution of sediments, strong of proximity to sediment sources and lithosphere age

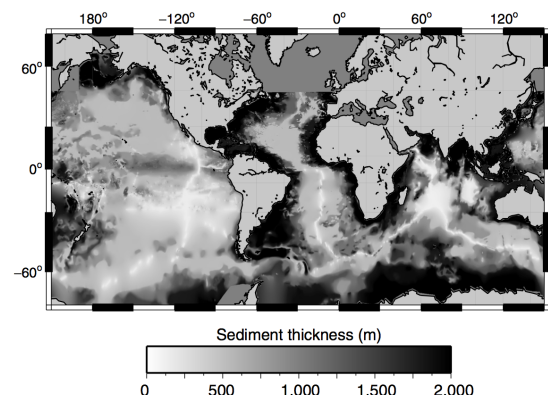
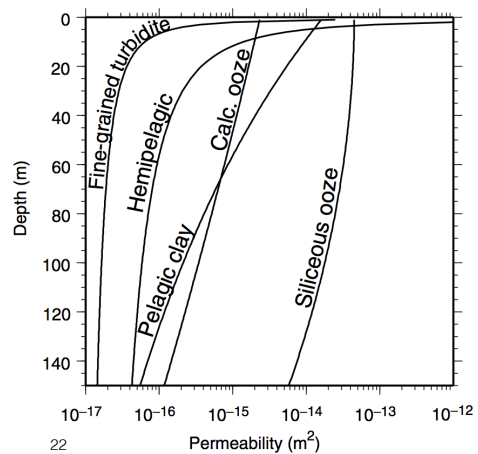


Fig. 6.2 Global distribution of sediment thickness (data from Divins, 2002). Sediment thickness data are compiled from ocean drilling results and reflection seismic profiles, and gridded with a spacing of  $5 \times 5'$ . Sediment thickness varies as a function of lithospheric age (distance from mid-ocean ridge), proximity to zones of high biological productivity, and proximity to terrigenous sediment sources. Sediment greater than 2,000 m thick, primarily on continental margins, is shown in black.

23

## Permeability of seafloor hydrothermal systems

- Permeability of fine-grained seafloor sediments decreases rapidly with increasing depth due to mechanical compaction
- Poorly constrained, sample recovery obviously difficult and in-situ measurement as well
- Permeability likely too low to allow convective fluid flow

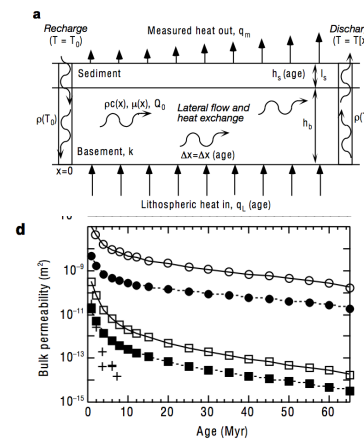


Spinelli ea (2004)

22

## Permeability of seafloor hydrothermal systems

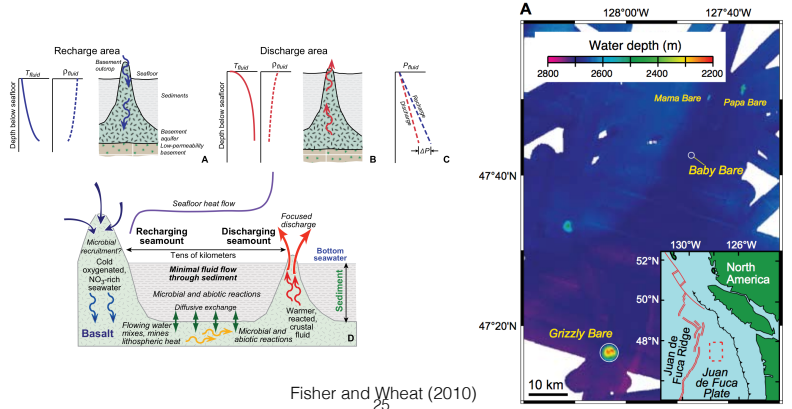
- Model of heat transport to explain difference observed and predicted (lithospheric) heat flow at ridge flanks
- all the model experiments needed much higher permeability than observed (bottom panel)
- can only be resolved if flow through discrete high permeability channels in upper oceanic crust, possibly through permeable pillow basalts/breccias in upper extrusive layer



Fisher & Becker (2000) Nature  
24

## Seafloor hydrothermal systems, case study:

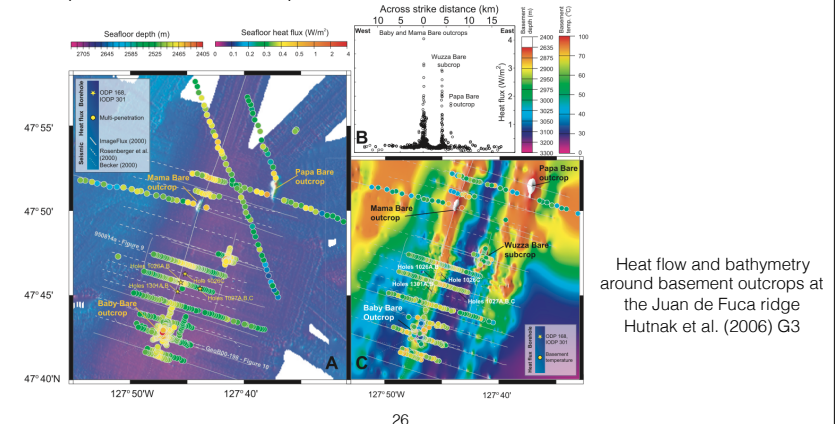
- One of the best studied hydrothermal systems & spreading ridges: Juan de Fuca ridge



Fisher and Wheat (2010)  
25

## Seafloor hydrothermal systems, case study:

- Strong heat flow focusing at basement outcrops in ridge flank (~3 Ma ocean crust)

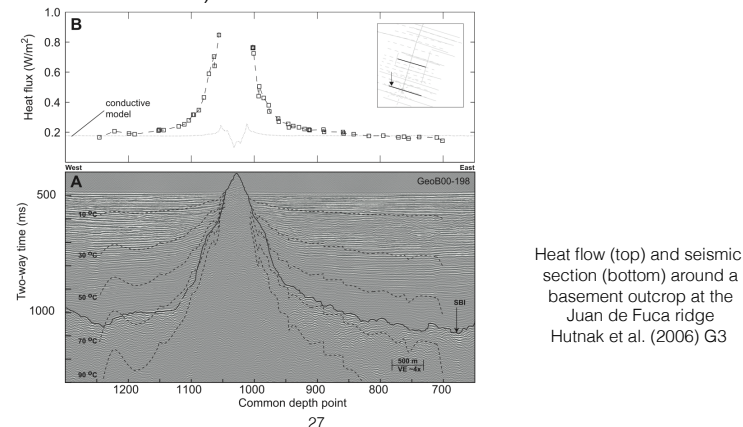


26

Heat flow and bathymetry around basement outcrops at the Juan de Fuca ridge  
Hutnak et al. (2006) G3

## Seafloor hydrothermal systems, case study:

- Strong heat flow focusing at basement outcrops in ridge flank (~3 Ma ocean crust):

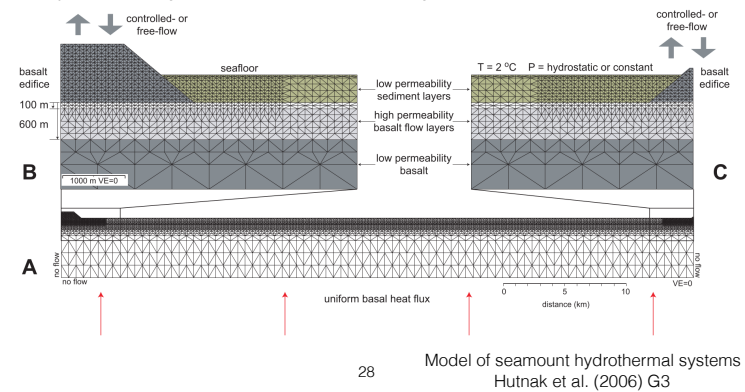


Heat flow (top) and seismic section (bottom) around a basement outcrop at the Juan de Fuca ridge  
Hutnak et al. (2006) G3

27

## Models of seafloor hydrothermal systems

- How do seafloor hydrothermal systems work?
- Numerical model of pair of seamounts/basement outcrops separated by wide area covered by sediments

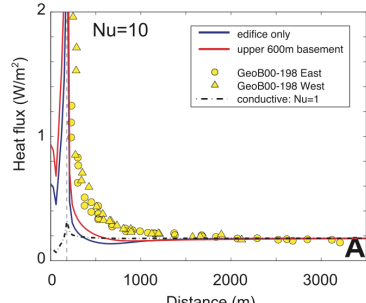


28

Model of seamount hydrothermal systems  
Hutnak et al. (2006) G3

## Models of seafloor hydrothermal systems

- Results: local thermal convection results in small scale convection cells in the seamount alone and cannot explain the width of the observed zone of high heat flow up to 1 km distance from the seamount

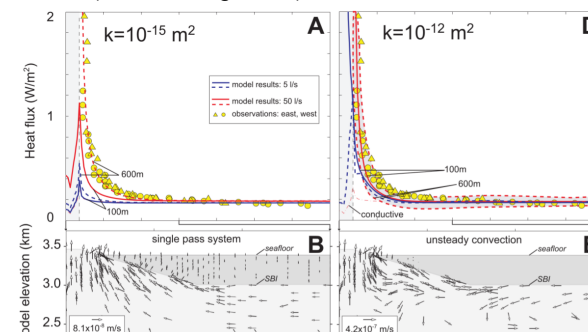


Model of seamount hydrothermal systems showing a misfit between local convective flow and observed heat flow data  
Hutnak et al. (2006) G3

29

## Models of seafloor hydrothermal systems

- Results: observation can be reproduced, but not by free-convection only. Recharge is forced by injecting fluid at the recharge basement outcrop (not shown). Background heat flow harvested by fluids from 50 km flow path is enough to reproduce localised heat flow anomalies.

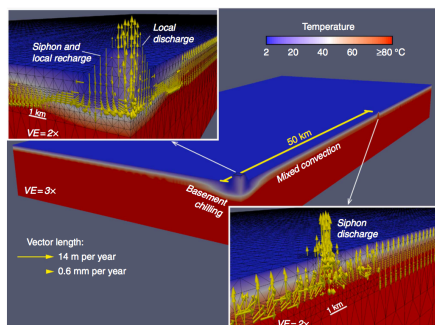


Model of seamount hydrothermal systems using low (left) and high (right) permeability for basement rocks  
Hutnak et al. (2006) G3

30

## Models of seafloor hydrothermal systems

- However, recent 3D models may have been more successful and simulate a hydrologic siphon that successfully transport water from seamount to seamount over 50 km, without inducing recharge
- Two-step process to establishing a seamount-seamount hydrothermal system:
  - Local thermal convection in each seamount. This on average cools the subsurface in each seamount. However, this effect is much higher for larger seamounts
  - Colder, denser water at large seamounts has a higher fluid potential, and will want to flow towards areas with a lower potential, such as smaller seamounts with a much lower rate of convection and higher temperatures
  - A "siphon" is established, with recharge of cold seawater at a large seamount, and discharge of water that has been heated up along the way in a smaller seamount
  - This process is self-sustaining once it is established



31

Winslow et al. (2015) Nature Comm.

## Models of seafloor hydrothermal systems

- Basement permeability of  $10^{-12} \text{ m}^2$  can explain observed high fluid flow and heat flow at basement outcrops
- Note that this is the opposite of what we see onshore, where sediments tend to show much higher permeabilities than crystalline rocks
- basement  $k$  of  $10^{-12} \text{ m}^2$ =equal to permeable sand > strongly fractured crystalline rocks. + positive feedbacks by dissolution?

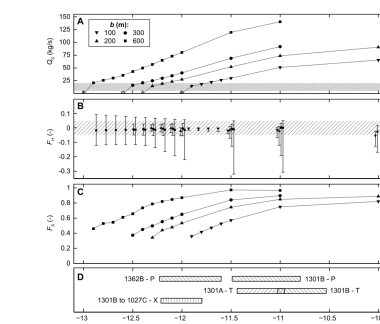
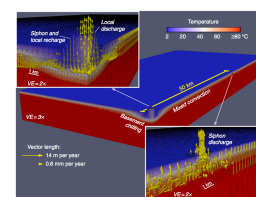


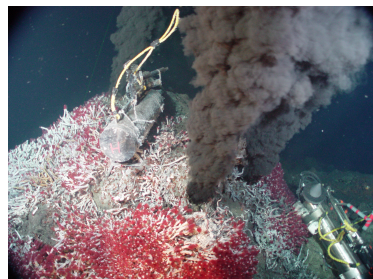
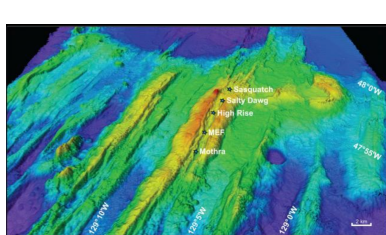
Figure 5. Results from AQTESOLV simulations and comparison with borehole data. (a) Siphon flow ( $Q_s$ ) versus aquifer permeability, with symbol type differentiating aquifer thickness. Each symbol represents a single simulation, run to dynamic steady state. The shaded area is the range of discharge rates estimated for Baby seamount [Thackeray et al., 1995; Winslow et al., 1998; Wheat et al., 2004]. Grey symbols are the highest values for the siphon, and the remaining symbols represent the range of fracture (f\_f) versus aquifer thickness permeability. The shaded area highlights simulations with  $f_f < 0.05$ , satisfying observational constraints. Filled symbols indicate the mean values for seafloor nodes in each simulation, and the error bars indicate the 25th and 75th percentiles of seafloor values. Symbols are shifted slightly left or right for clarity.

Winslow et al. (2016) JGR

32

## Models of seafloor hydrothermal systems: ridge axis

- Juan de Fuca ridge black smokers:

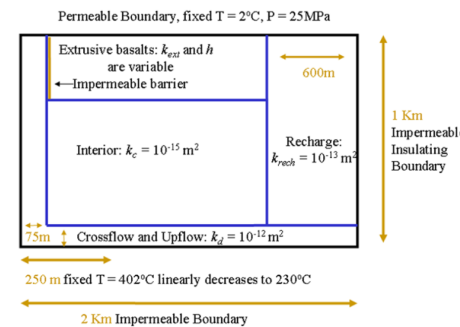


Source: NOAA

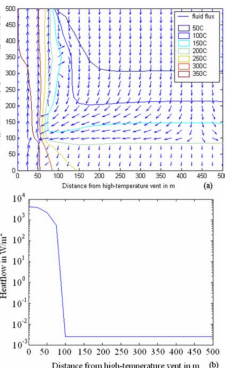
33

## Models of seafloor hydrothermal systems: ridge axis

- Convective models require a basal high permeability layer:



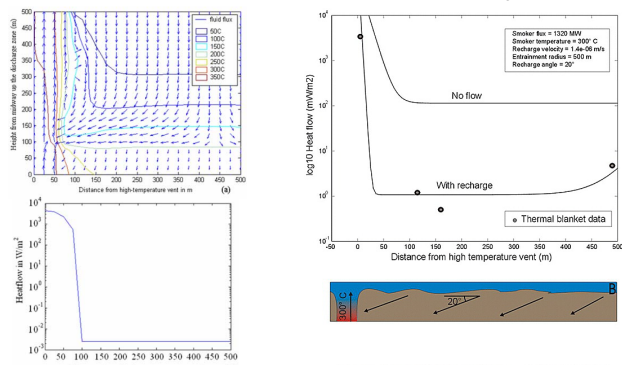
simple 2d convection model of a black smoker, Lowell et al. (2007) G3



34

## Models of seafloor hydrothermal systems: ridge axis

- Actual heat flow data to constrain models relatively scarce:



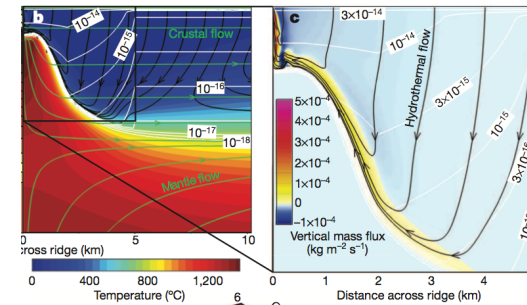
THERMAL BLANKET DATA - AND MODEL

simple 2d convection model and heat flow data near a black smoker at Juan de Fuca ridge, Lowell et al. (2007)

35

## Models of seafloor hydrothermal systems

- More spectacular model simulations of high temperature systems on ridge axis
- Extremely challenging numerically, high temperatures, multiple phases (critical fluids, vapour), changes in permeability due to temperature changes and hydrothermal alteration, etc...
- Extremely challenging numerically, 1 model run takes several weeks on a cluster

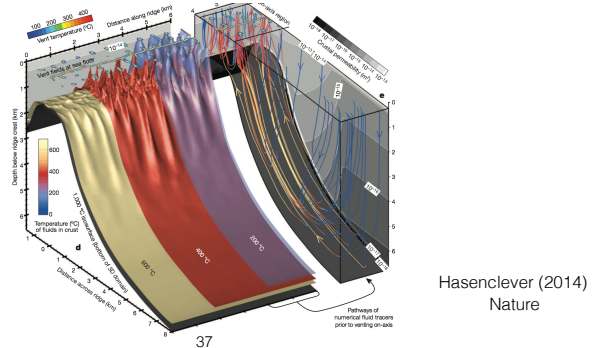


Hasenclever (2014)  
Nature

36

## Models of seafloor hydrothermal systems

- More spectacular model simulations of high temperature systems on ridge axis
- Seems to reproduce first order effects with some success, high temperature vents (black smokers), pervasive hydrothermal alteration, high fluid inclusion temperatures observed in oceanic crust (>500 °C)
- Imposed high k layer at base of crust due to thermal cracking. needed to reproduce observations, but still speculative

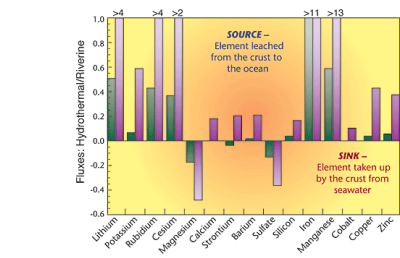


## Impact of oceanic hydrothermal systems

- Oceanic hydrothermal systems are responsible for ~ 25% of global heat flux
- Total water flux poorly constrained to oceans, but may be higher than total river flux to oceans
- Hydrothermal solute fluxes are much higher than river input into oceans for many elements
- Hydrothermal alterations strongly alters the composition, density and strength of the oceanic crust, and may be essential to keep plate tectonics going (ridge push, subduction)

Table 1 Heat and volume fluxes associated with seafloor hydrothermal circulation		
(I) Summary of global heat fluxes		
Heat flux from the Earth's interior	43 TW	
Heat flux associated with ocean crust	32 TW	
Seafloor hydrothermal heat flux	11 TW	
(II) Global hydrothermal fluxes: heat and water		
Heat flux (TW)	Water flux ( $10^{14}$ g year $^{-1}$ )	
Axial flow (0-1 Ma)		
All flow at 350 °C	2.8	5.6
20% @ 350 °C (0.5 °C)	2.8	375
Hydrothermal plumes (20%)	-	~11 000
Off-axis flow (1-85 Ma)	7 ± 2	2000-10 000
Global riverine flux	-	~4000

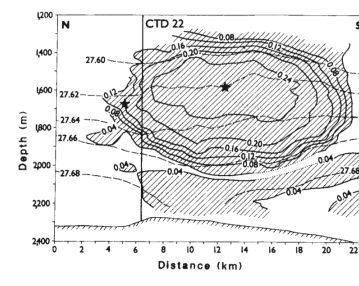
Source: German (2014) Treatise on geochemistry



39

## Episodic hydrothermal plumes

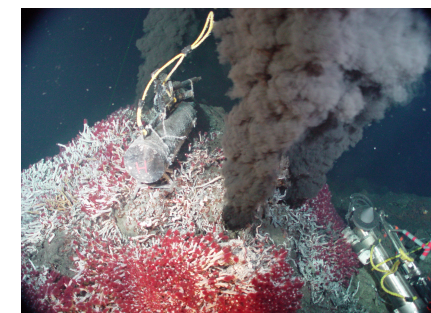
- Juan de Fuca ridge was the location of largest recorded hydrothermal plume, with a volume of 130 km<sup>3</sup>
- no explosive volcanic origin, no pyroclastic fragments, composition typical of hydrothermal fluids
- =annual heat and silica output of >200 black smokers
- cause still unknown...



Measured temperature anomaly in the ocean near the Juan de Fuca ridge. Baker et al. (1987) Nature  
38

## Impact of oceanic hydrothermal systems

- High-energy environment that hosts unique lifeforms and ecosystems that are not dependent on oxygen and photosynthesis, but use reduced sulfur instead
- Seafloor hydrothermal systems may have enabled the emergence of life on our planet



Source: NOAA, <http://www.pmel.noaa.gov/eoi/multimedia.html>

40

# Continental hydrothermal systems and early life?

- Alternative theory that life started in silica dominated terrestrial hydrothermal system instead of seafloor hydrothermal vents:

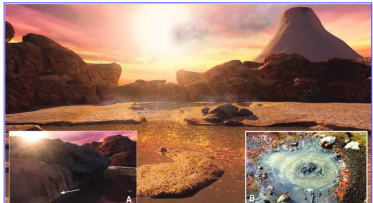


FIG. 2. An artist's conception of a geyser-driven Italian volcano hydrothermal system in which cycles of evaporation and dehydration can occur. **Inset A** shows a ring of dried solutes on the mineral surfaces at the edge of a fluctuating pool. **Inset B** shows a boiling pool associated with a hot spring site on Mount Mutnovsky in Kamchatka, Russia. (Art credit: Ryan Norkus; Photo credit: Tony Hoffman.)

Deamer & Deamer (2019) Astrobiology

Geyser and deposits containing thermophilic microbes at Beowawe  
White et al. (1998) USGS report  
41

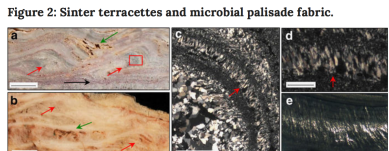


Figure 2: Sinter terracettes and microbial palisade fabric.  
Scale bar measurements indicated. (a) Dresser terracettes (red arrows) with preserved primary porosity (green arrow) and a horizon containing Dresser stratiform geyserite (black arrow). Scale bar, 1 cm. Inset box of c. displays palisade fabric. (b) >1,800-year-old sinter

Presumed signs of early life in 2.5 billion year old 'geyserites'  
from the Pilbara region, Australia  
Djokic et al. (2017) Nature Comm.



Figure 3: Geyser erupting from a hole in the ground.

## Summary

- Significant mismatch between observed and predicted heat flow in <65 Ma old ocean crust in models constrained by independent variables (depth, gravity)
- Difference can be resolved by highly focused advective heat transport by fluids that facilitates ~30% of the total heat loss in the oceanic crust
- Spreading ridges host high temperature systems (>350 °C), black smokers. Can be explained by thermal convection, but need a poorly constrained high permeability ( $k \sim 10^{-12} \text{ m}^2$ )
- Ridge flanks: lower temperature (100-200°C) vents at widely spaced outcrops of basement rocks between sedimentary cover. Long range (tens of km) fluid flow between seamounts. Can potentially be explained by combination of thermal convection and siphon formation due to difference in convection and temperature between different seamounts
- Impacts of oceanic hydrothermal systems: ~25% of global heat flux, dominant effects on ocean chemistry, unique ecosystems and may have helped to start life on our planet